East European Journal of Physics. 2. 399–410 (2026)
DOI: 10.26565/2312-4334-2026-2-44 ISSN 2312-4334

AN IN-DEPTH FIRST-PRINCIPLES STUDY OF THE STRUCTURAL, STABILITY, ELECTRONIC, THERMODYNAMIC, AND OPTICAL CHARACTERISTICS OF TWO-DIMENSIONAL BiBrO

Yadgar Hussein Shwan
Physics Department, College of Education, University of Sulaimani, Sulaymaniyah 46001, Kurdistan Region, Iraq
**Corresponding Author e-mail: yadgar.shwan@univsul.edu.iq*
Received March 7, 2026; revised May 16, 2026; accepted May 18, 2026

This study leverages DFT within the GGA framework to provide a thorough calculate of the stability, electronic properties, thermal performance, and optical responses of 2D BiBrO. The computed formation energy, along with phonon calulation findings and AIMD results, verifies the stable structural, dynamical and thermal stability of the BiBrO system. The 2D BiBrO material exhibits semiconducting behavior with a band gap of 2.42 eV, as confirmed by electronic band structure analysis. Optical properties analysis of BiBrO reveals powerful visible and ultraviolet (UV) light interaction, which supports its applications as a solar energy storage device. The large ability of BiBrO to store thermal energy is due to high heat capacity, because BiBrO has a greater phonon density of states. The entropy rises proportionally to the temperature which means that there is additional atomic disorder and more accessible microscopic states. Furthermore, the increase in entropy and the plateau in heat capacity at high temperatures imply a change toward a more disordered state, while yet allowing for effective thermal energy absorption. The low lattice thermal conductivity and smaller phonon group velocity of BiBrO are the characteristics that render the material useful in thermal insulation, while maintaining structural stability. These findings give critical information regarding how BiBrO may be used in energy storage systems as well as thermal barrier.

Keywords: *2D BiBrO; DFT; Electronic characteristics; Lattice thermal conductivity; Optical characteristics; Stability*

PACS: 71.15.Mb, 73.22.-f, 78.20.-e, 63.20.dk, 65.80.-g, 66.70.-f

1. INTRODUCTION

Since the discovery of Graphene in 2004, there is a significant interest in the two dimensional materials. Due to their small dimensions, which causes reduced dimensionality, their electrical, optical, and catalytic properties are promising platforms with respect to high-level electronic and energy applications. The materials covered in this category are quite diverse with Hexagonal boron nitride (h-BN), Hexagonal boron-carbon-nitride (B- C-N) transition metal oxides (TMOs), transition metal dichalcogenides (TMDs), and metal halides each with its own structural and physicochemical properties to support many technological applications [1–5]. In recent years, much research effort has been devoted to the study of novel two-dimensional materials for various applications such as spintronics, chemical and biological sensing, supercapacitors, solar cells and lithium-ion batteries. [6, 7].

The crystal structure of transition metal dichalcogenides (TMDs) is usually considered MX2, and is layered, which is most often implemented in two dimensions (2D). These materials have a large variety of physical properties such as semiconducting, superconducting and metallic. The MX2-type layered materials, including graphite (i.e., stacked sheets of graphene), include strong covalent bonds in each layer, and relatively weak van der Waals (vdW) forces between individual layers in their bulk phases. In the recent past, there is a proposal of a new category of MX-type 2D material and there has been a lot of concern as these materials have shown promising and wide-ranging physical characteristics [8–10]. Bismuth triiodide (BiI_3) is a layered semiconductor that has attracted considerable attention for optoelectronic and photovoltaic applications due to its suitable band gap and strong optical absorption. First-principles density functional theory (DFT) studies, demonstrated that bulk BiI_3 consists of weakly bonded van der Waals layers, making the exfoliation of a stable BiI_3 monolayer energetically feasible. Their calculations further revealed that monolayer BiI_3 exhibits semiconducting behavior with a band gap appropriate for visible-light absorption and a high absorption coefficient in the visible region, highlighting its potential for ultrathin solar cells and photodetectors [11–13]

Bismuth bromide oxide (BiOBr) crystallises in a layered matlockite-type tetragonal form of (space group P4/nmm). Being a part of the (BiOX, X = Cl, Br, I) group. BiOBr is a semiconductor, which has an indirect band gap of about 2.46 eV, which allows it to have a lot of absorption in the visible-light portion. Due to these structural and electronic properties, BiOBr has drawn a lot of attention to be used in photocatalysis, optoelectronics and photovoltaic devices [14–16]. These properties of the BiBrO provide a promising future because of its layered structure. This is a structure whereby a two dimension structure can be formed due to the weak van der Waals forces , which are used to stacked the layers. The layers are exfoliable to 2D nanosheets, as is the case with graphene which is made of graphite. This makes BiBrO a large surface area 2D material [17]. Theoretical calculations of a BiBrO singlayer with uncharacteristically high thermal stability as verified by dispersion-phonon calculation. In addition, the material is semiconducting and has a wide band gap [18].

Cite as: Y.H. Shwan, East Eur. J. Phys. 2, 399 (2026), https://doi.org/10.26565/2312-4334-2026-2-44

The crystal structure of BiBrO has not been fully analyzed, and its complete characterization remains limited. Further investigations are necessary to achieve a comprehensive understanding of the BiBrO structure. This study employes (DFT) computations to thoroughly calculate the fundamental features of BiBrO in its tetragonal crystal form. The present study offers a thorough investigation of both the low- and high-temperature behavior, in addition to the thermal stability of BiBrO, using ab initio molecular dynamics (AIMD) simulations. The formation energy is calculated to assess the energetic stability of the atomic configuration. Additionally, the electronic properties of BiBrO are analyzed in detail through an examination of its band structure and partial density of states (PDOS). The optical properties are further examined by calculating the real and imaginary components of the dielectric function, as well as the refractive index, reflectivity, absorption coefficient, and optical conductivity. The thermal characteristics of the material were comprehensively analyzed through heat capacity and entropy calculations, followed by investigations of the phonon-band structure to assess its dynamical stability. Bismuth oxybromide (BiOBr) demonstrates relatively low thermal conductivity, positioning it as a promising candidate for thermal insulation applications. Its capacity to restrict heat transport, along with its structural stability, underscores its potential in energy-related technologies.

The rest of this paper is arranged as follows. Section 2 explains the computational methods used in this investigation. Section 3 delves further into the structural, electrical, dynamical, thermal, and optical aspects of the researched atomic configurations. This section focuses on the material's electrical properties, thermal transport characteristics, and interaction with electromagnetic radiation. Finally, Section 4 summarizes the main findings and highlights the study's significant conclusions.

2. COMPUTATIONAL APPROACH

We examine a two-dimension unit cell of BiBrO with space group $P4/nmm$ consisting of 6 atom. Quantum espresso utilizes the projector augmented wave (PAW) framework for conducting first-principles calculations with DFT. Besides this, the exchange-correlation effects were modeled on the basis of the generalized gradient approximation (GGA) with the use of the Perdew Burke Ernzerhof functional (PBE) formulation. A convergence test establishes the suitable kinetic energy cutoff for Brillouin zone sampling through testing. A combination of $11 \times 11 \times 5$ Monkhorst-Pack k-point grid and 50 Ry plane-wave cutoff is used as the computational parameters. None self consistent field (*nscf*) calculations require a denser k-point grid of $50 \times 50 \times 5$ for their execution. Using the relax and vc-relax modes structural relaxation processes the unitcells and atomic arrangements to find optimal structures which can be analyzed well. The relaxation energy reaches convergence at 2.72×10^{-7} eV [**?**, 19].

The AIMD simulation run tests thermal stability on a unit cell maintained at 300 K for 5 ps. Structure undergo analysis of their electronic and optical characteristics when they reach full relaxation, where stress are less than $6{\times}10^{-4}$ eV/Å. Phonopy program calculates dynamic stability, entropy and heat capacity using phonon-related parameters such as frequencies and density of states (DOS). Thermal conductivity of lattice was determined by iteratively solving the phonon Boltzmann transport equation using phono3py, using a $20 \times 20 \times 2$ q-mesh. XCRYSDEN and BURI 1.3. are used to visualize and design structures, as well as to improve our understanding of material characteristics by assuring correct modeling and guiding investigations [21–23]

3. RESULTS

In this part, the findings on the geometrical, stability, electrical, optical, and thermal characteristics of the 2D structure of BiBrO are provided.

3.1. Geometric properties

Before we begin understanding BiBrO structure we must determine its basic shape. The BiBrO structure visualization displays top and side views in Fig. 1. BiBrO crystallizes in the tetragonal $P4/nmm$ space group and takes on a structure similar to that of Matlockite. The crystal is made up of a single BiBrO unit cell layer in two dimensions. The Bi^{3+} cation interacts with four equivalent O^{2-} atoms and four equivalent Br^{1-} atoms, displaying a fourfold coordination environment. The measured lengths of the Bi-O and Bi-Br bonds are 2.33 Å and 3.19 Å, respectively. Matlockite compounds are characterized by a stable layered framework formed by the coordination of each O^{2-} anion to four equivalent Bi^{3+} atoms to form a mixture of corner and edge-sharing OBi_4 tetrahedra. The Br^{1-} anion is four-fold coordinated and bonds to four equivalent atoms of Bi^{3+}. The structural properties were evaluated with the help of the optimized lattice parameters (a, b, and c) that determine the size of the unit cell and the arrangement of atoms in the BiBrO crystal structure [24].

Accurate simulation models for BiBrO electronic and thermal as well as optical characteristics require an precise descriptions of its geometric features including unit cell dimensions, lattice and bond length parameters. Geometric variation factors produce substantial effects on both electronic band structure together with phonon dispersion and optical response. After fully relaxed structure. The best lattice values are $a = 3.93$Å, $b = 3.93,$ Å which proves the tetragonal symmetry in the plane. To avoid unwanted interlayer interactions in the two-dimensional model, a vacuum gap of $c = 8.39$ Å was added along the out-of-plane direction, their description outlines how atoms are arranged within a unit cell structure. The physical properties of the BiBrO are evaluated using relaxation structure-parameters. The observed results matched previously recorded data [25, 26].

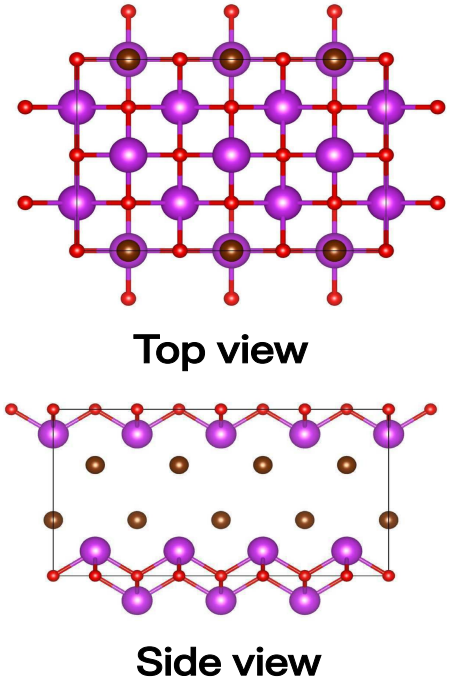

Figure 1. 2D BiBrO structure is shown from the top view (upper panel) and side view (lower panel).

3.2. Stability

Multiple approaches are used to investigate the stability of the BiBrO structure, including calculating formation energy and executing molecular dynamics simulations in combination with phonon dispersion analysis. An important thermodynamic quantity called formation energy (E_f) measures changes in energy during the process of creating compounds from their most stable standard state elements. When the formation energy becomes negative it indicates that the material's creation process remains energetically stable. Finding positive formation energy means decreased thermodynamic stability and increased disposition to decompose the material [27]. The study of BiBrO indicates stable structure due to its negative energy (-1.63 eV at a = 3.85Å), as is illustrated in Fig. 2(a).

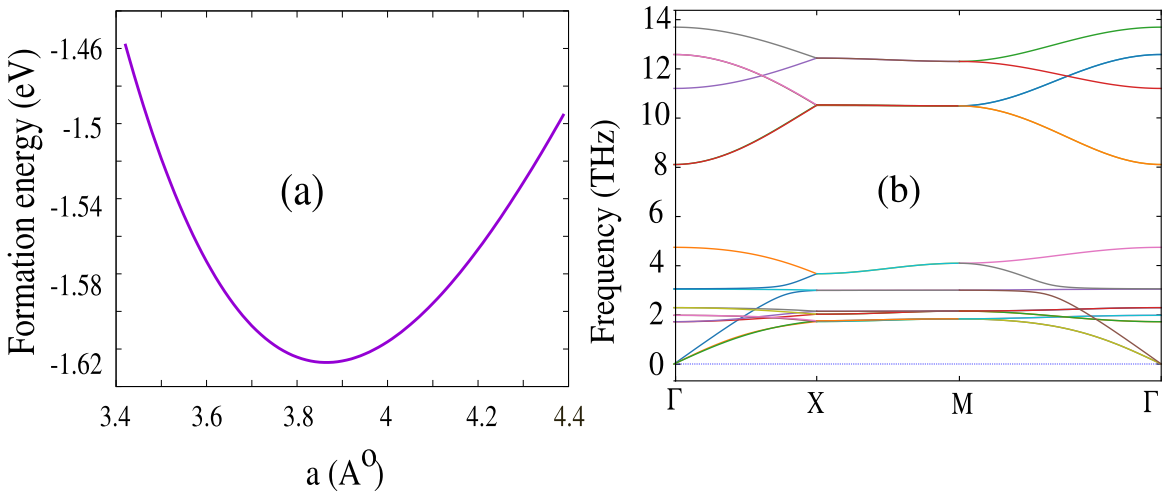

Figure 2. "Formation energy of 2D BiBrO as a function of its lattice constant (a), Phonon dispersion curve of 2D BiBrO(b).

The Fig. 3 presents the findings of the AIMD simulation that studied the thermal stability of 2D BiBrO at 300 K. The simulation duration consisted of 5 ps at each 1.0 fs time step. The temperature pattern varies minimally during the simulation because heat transport inside the 2D BiBrO structure is restricted at that temperature. Results from these simulated normal environmental assessments is shown that the structure maintained a stable state. The testing revealed neither substantial damage nor bond disruption to the structural makeup. The energy fluctuations per atom shown in Fig. 3(b) confirm this observation by staying under 0.17 Ry, which matches other reported DFT studies.

The simulation results confirm that no major energetic changes took place inside the BiBrO system during the computational period. The lack of observable structure deformation exists at each time step indicating varying temperature points [23, 28, 29].

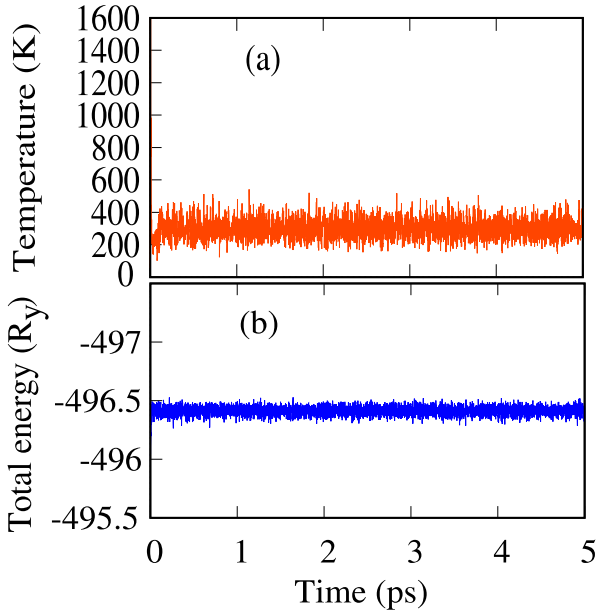

Figure 3. AIMD simulation for 2D BiBrO,(a) temperature,(b) total energy, as a function of time.

The frequencies of phonons identify key characteristics about material stability and physical behavior. Studying phonon dispersion is critical for understanding basic macroscopic properties of materials, such as their specific heat and thermal expansion responses. Phonon modes whose frequencies fall within the lower range are known as soft modes which have direct links to structural phase transitions, while the inspection of Fig. 2(b) demonstrates that BiBrO exhibits dynamic stability by showing no formation of imaginary phonon modes throughout the Brillouin zone which proves its resistance to spontaneous lattice distortions. Both transverse acoustic and longitudinal acoustic phonon branches show linear dispersion near the Γ point which defines the stable crystalline material behavior for sound wave propagation through the lattice. The flexural acoustic phonon branch has a parabolic form around the Γ point, indicating two-dimensional shapes material characteristics. The identical phonon dispersion pattern occurs routinely in other 2D materials such as graphene alongside transition metal dichalcogenides. The analysis of phonon dispersion shows that BiBrO acoustic branch frequencies stay below 2 THz which produces values much lower than h-BN and other two-dimensional materials.Due to the low frequencies and present heavy atoms (Bi and Br). This causes BiBrO naturally an inefficient heat conductor, therefore it may be used as insulation material [30–32]

3.3. Electronic properties

We first analyzed BiBrO's thermal stability. Then, we computed the electronic properties of BiBrO. It is mostly determined by the band structure and (PDOS) throughout the chosen path Γ→X→M→Γ. PDOS and bandstructure are related to the same energy level with the energy of Fermi set to be zero, they are depicted in Fig. 4 and Fig. 5. The electronic band structure of BiBrO shows that its valence band maximum (VBM) appears near the M point and its conduction band minimum (CBM) exists at the Γ point. Bandgap indirect behavior is confirmed by the VBM and CBM regions showing spatial separation as this reveals a momentum-changing electron transition between valence and conduction bands. Knowledge about this behavior stands essential for optical characterization because it influences how electrons interact with light. The calculated energy bandgap of 2.42 eV in Fig. 4 might be underestimated since the study uses GGA-PBE approach. The calculated 2.42 eV bandgap operates within the spectrum of visible light, which stands crucial for solar energy applications. The material exhibits a unique quality that makes it desirable for photovoltaic uses [33, 34].

BiBrO shows a non-flat band structure indicating that electrons display substantial dispersion together with non-localization across energy levels when momentum changes. Across the Brillouin zone, the band edges fail to match in alignment, which results in the formation of non-flat band structures. The change in energy level positions occurs as momentum shifts through the bands, the hybridization of atomic orbitals together with complex bonding relationships between Bi, Br, and O elements produces this variation. Lower BiBrO symmetry causes increased energy band dispersion through diminished degenerate energy states which generates extensive band gaps. The crystal structure demonstrates incomplete symmetry characteristics because of structural imperfections [35, 36].

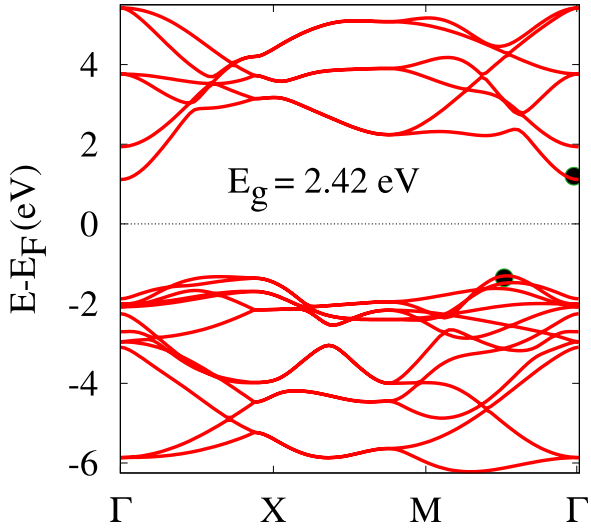

Figure 4. Electron band structure of 2D BiBrO with the Fermi energy referenced to zero.

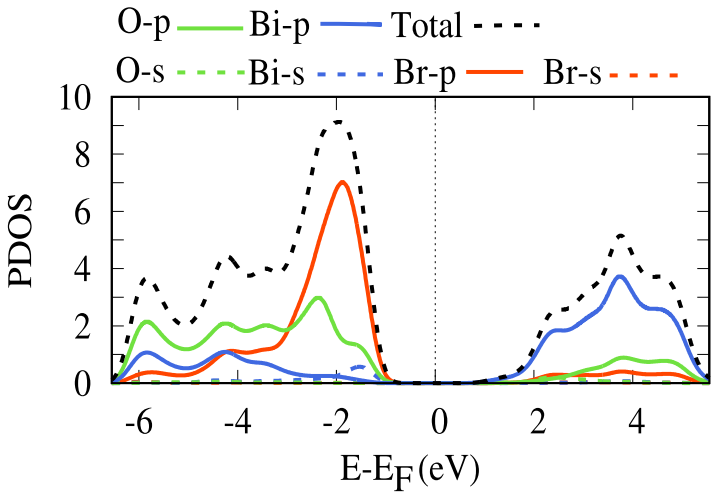

Figure 5. Total and (PDOS) of 2D BiBrO structure.

The (PDOS) analysis investigated orbital participation from each constituent atom across a -6.25 to 5.5 eV energy range of the band structure. The graphical representation of this analysis shown in Fig. 5 provides critical understanding of the bonding features in the material. The valence band predominantly contains Br-p orbitals because of extensive atomic interactions throughout the bismuth-oxygen-bromine system which produce an ionic bond framework. Bi-p orbitals contribute extensively to electronic as well as optical properties in the CB phase of BiBrO. The substantial electronic character gap between Br, Bi and O elements proves the ionic nature of BiBrO bonding. The material exhibits a band gap spanning (-1 to 1.4) eV leads to zero PDOS because electronic states are not allowed during this interval.

The PDOS study reveals that the Bi-p and Br-p orbitals, that involved in the interaction, remain mainly different. This implies that there is minimal hybridization of these orbitals, confirming that the interaction between bismuth and bromine remains primarily ionic or weakly covalent in nature. The separate orbitals function independently while avoiding mixing so they maintain their original characteristics which results in localized states distribtion. Cl-p orbitals have a smaller PDOS peak than Br-p orbitals, indicating that Br participates substantially more to the bond-intraction within the investigated energy range. This implies that Br-p orbitals are more delocalized or actively engaged in the electronic structure, while Cl-p orbitals might seem more localized or only partially participating in bonding interactions. The interactions among these orbitals, as well as the spatial configuration of atoms, result in diverse contributions to the levels of energy at various k-points in the Brillouin zone. The BiBrO structure exhibits an indirect band gap due to the appearance of the VBM and CBM along the M-Γ route [37]

3.4. Optical characteristics

This section discusses the optical characteristics of 2D BiBrO, with an emphasis on essential parameters such the dielectric function,ε, absorption coefficient,α, and optical conductivity σ. These values are computed using the Random

Phase Approximation (RPA) method on the Brillouin zone with a tighter k-point grid across the energy range 0 to 10 eV. These characteristics explain how the material reacts to incident electromagnetic spectrum and are essential for determining its optical applications such as solar energy harvesting. The dielectric response changes with the energy of photons through electric fields applied both parallel (E_x) and perpendicular (E_z) as seen in Fig. 6. The results from both x and y-polarized electric field testing show similar which demonstrate symmetry optical behavior of BiBrO. The material generates dissimilar polarization patterns along the x-axis and z-axis because of its lowest anisotropic structure [38, 39].

The real part Re(ε) is the active component related to the response of structures to electrical energy storage. The static dielectric constants at the energy of a zero photon are 5.8 for E_x and 6.9 for E_z. This implies that BiBrO has a high polarisation behaviour, which indicates that it is easily polarizable, given that its constituent atoms are relatively less sensitive to external electric fields. Around 3 eV the material exhibits its highest optical response and therefore shows relatively high dielectric values because of the limited anomalous dispersion at this energy, in agreement with the Kramers–Kronig relations. This would mean high potential for energy storage in electricity. Around 5 eV, the material enters a plasmonic regime defined by the negative value of the Re (ε) due to the presence of collective oscillations of electrons. This is where the material no longer accommodates propagating waves, highlighting its potential for plasmonic uses [40, 41].

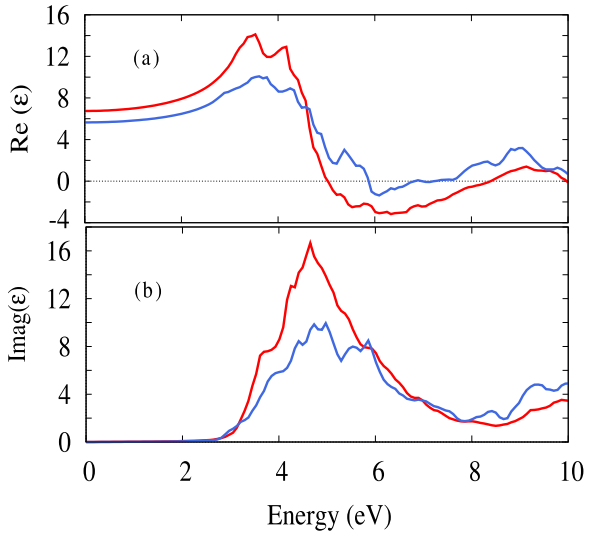

Figure 6. Re (ε) (a) and imag (ε) (b) parts of the dielectric function of 2D BiBrO under external electric fields applied parallel (E_x, red) and perpendicular (E_z, blue) to the plane.

The imag (ε) of the dielectric has a different response to various frequencies (viewed in Fig. 6,(b)). Imag(ε) reflects the material's ability to absorb energy. Its absence in the 0–2.41eV range suggests that the optical bandgap, which is consistent with the electronic bandgap. Significant peaks at high energies are indicative of the presence of interband transitions and a high joint density of states in these areas of frequencies. Imag(ε), the imaginary portion of the dielectric function, is linked to the material's shielding electromagnetic radiation capabilities via screening processes. Shielding efficiency enhances with higher Imag(ε), whereas lower Imag(ε) values result in poorer shielding. Surprisingly, the two absorption and screening performance are strongly correlated with the material's electronic structure and optical response. For both field orientations, both the real and imaginary parts of the dielectric function exhibit the same increasing tendency from visible region to deep UV region. Such behaviour indicates that the material is a good candidate for energy storage and UV photo detector application [24, 42].

Optical conductivity, σ, measures the ability of a material to transport electric currents when a material is exposed to an optical field. The optical conductivity has pronounced variation with photon energy as can be seen in Fig. 7. One important observation is that the optical conductivity σ is essentially zero in the energy range from (0 to 2.41) eV owing to a limited number of electronic states capable of taking part in optical transitions, Also, it can be described as the optical band gap. Over this threshold, there is a steep rise in the optical conductivity level which is indicative of quick onset of inter band transitions. This is a typical property of a wide band-gap semiconductor in which much energy is necessary to move electrons from the valence band to the conduction band. The photon energy which exceeds the band gap plays an important role in deciding the overall transition strength and the participation of most interband transitions. This data provides an insight into the patterns of the charge transport, the knowledge that is needed by the developers for the generation of the solar energy as well as the photodetectors, and also for the design of the optoelectronic systems [43, 44]

The way light travels through a substance is described by the dimensionless refractive index (n). It affects the dispersion of various wavelengths and establishes the phase velocity of light in the medium. The way the refractive index behaves, as seen in Fig. 7, gives insight into how electromagnetic waves interact with the material's electronic structure, especially how light is bent and slowed as it travels through. At zero photon energy, the material's stationary refractive

index (n) is 2.56 which pointed to a significant response to external electric field. Initially the refractive index increases slightly as photon energy increases where in other words is a drop in phase velocity of light. This tendency is typical of normal dispersion in transparent zones. However at about 4 eV the refractive index gradually decreases, this drop is related to the photon energy surpassing the material's band gap, resulting in increasing absorption and eventually saturation, which decreases the material's capacity to further slow down light [45, 46].

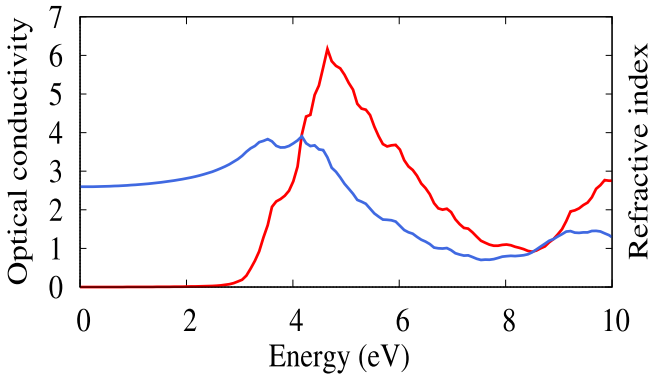

Figure 7. Optical conductivity (red) and Refractive index (blue) of 2D BiBrO in external electric field.

The absorption coefficient,α, defines the capability of a material to absorb photons depending on the photon energy (see Fig. 8). In extremely low photon energies, α is almost null because photons lack sufficient energy to spark electrons out of the VB to the CB. As the energy of photons approaches the band gap, α dramatically goes up, corresponding to a rise in Im(ε) owing to greater interband transitions, suggesting the start of substantial light-matter interaction. The capability to sense light from visible to Ultraviolet range as indicated by the absorption curve, is essential for opto-device applications. BiBrO exhibits intense absorption in the visible and deep-UV region, which suggests that it can serve as a highly effective light harvester and converter for a large range of light producing electricity. The absorption coefficient can therefore fall at very large photon energies, either because of a diminished joint density of states or because the transitions over step to the primary absorption edges themselves. Also, many-body effects, excitonic interactions and phonon scattering may affect on the absorption behavior but their roles are stronger in near the band edge and weaker at high energy [47].

The reflectivity of BiBrO is displayed in Fig. 8. From 0.0 eV to 2.8 eV, the reflectivity has a value of nearly 19%. At low photon energies (below the band gap), the free-electron dielectric response is weak. This means the material doesn't effectively reflect light, leading to very low reflectivity in that range. As photon energy increases above the band gap, reflectivity rises-potentially reaching values as high as 41% on average. This is because electrons can oscillate more strongly in response to the light. The reflectivity can be reduced to levels almost reaching zero at hight frequency. At this photon energy, the incident light is extremely transparent through it, as reflection is suppressed and absorption is negligible. Provided that this happens at around 8 eV, the material would effectively look transparent in that very limited ultraviolet wavelength. From this analysis, this material can be used as shielding in the UV range [48, 49].

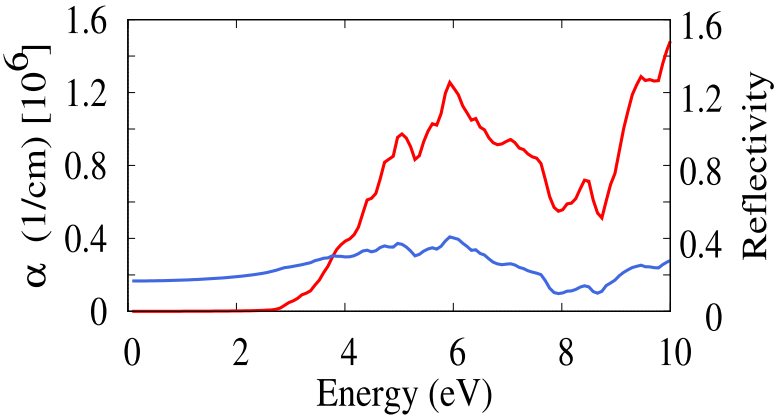

Figure 8. The absorption coefficient,α, (red) and reflectivity (blue) of BiBrO in external electric field.

3.5. Thermal properties

After verifying thermal stability. At intermediate high temperature ranges, we analyze BiBrO's thermal properties through temperature-dependent measurements of heat capacity C_V, entropy and phonon density of state which are displayed

in Fig. 9, Fig. 10. The heat capacity of a substance is defined as the ratio of heat absorbed to temperature change. Entropy measures a number of possible microscopic arrangements of the system and this is measured by entropy. The graph shows how a material's heat capacity and entropy vary with temperature (red and blue lines, respectively). At lower temperatures, both heat capacity and entropy gradually rise because the number of low energy vibrational states grows, according to quantum statistics. The C_V shows a distinct plateau from 300-1000 K, suggesting that the thermal energy needed to increase the temperature becomes almost independent of temperature. This behavior indicates that BiBrO is approaching the classical Dulong-Petit limit, where most lattice vibrational modes become fully thermally activated. As a result, further increases in temperature do not significantly enhance the phonon contribution to the heat capacity, which reflects the saturation of vibrational degrees of freedom. At 1000 K the value of C_V is 24.66J.K.mol per atom, nearly close to the Dulong-Petit limit as the phonon modes become mostly completely saturated [45].

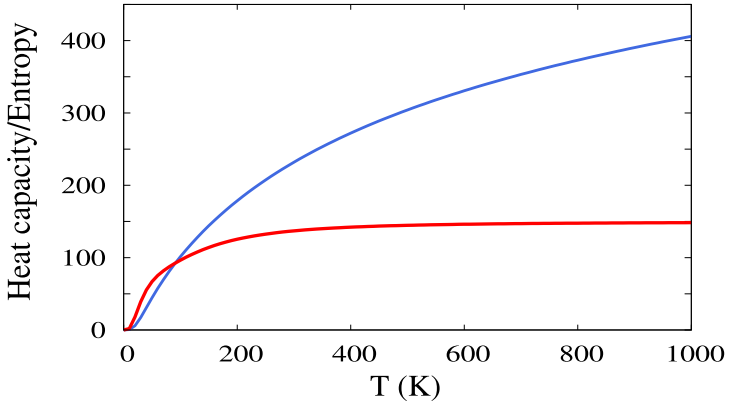

Figure 9. Capacity of heat(red) and entropy (blue) as a function of temperature of BiBrO.

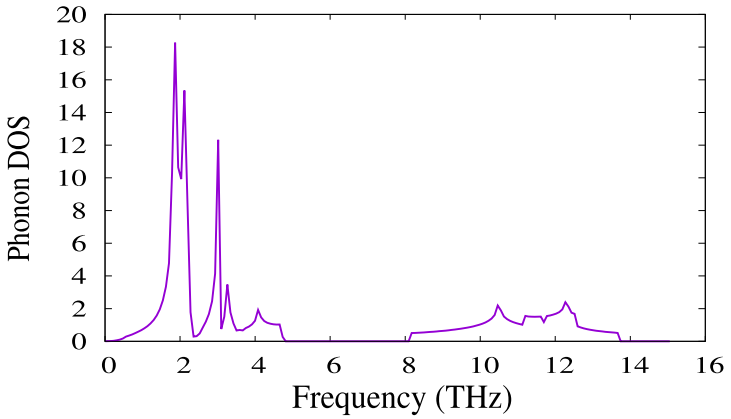

Figure 10. Calculate Phonon DOS of BiBrO.

Much like the blue curve of entropy, the entropy curve is rising with temperature but the rate of increase slows at high temperatures as the system gains more thermal energy, and the system is approaching maximum disorder. This is in line with the third law of thermodynamics.

As temperature approaches absolute zero, entropy tends to a finite constant (often zero for a perfect crystal), consistent with the Third Law of Thermodynamics, while the heat capacity vanishes because quantum mechanics restricts thermal excitations-only the ground state remains populated, leaving no accessible energy states to absorb heat. Conclude, the propagation of phonon, the major heat carriers in BiBrO material, is interrupted by the temperature induced disorder. Phonons are essentially vibrations of atoms in the material which are quantized. In the case of well-ordered atomic arrangement, These vibrations may effectively propagate through the lattice and thermal energy may be propagated. In a more disordered form, however, as is found in BiBrO at higher temperatures, the disordered atomic sites serve as scattering centres of phonon. These collisions can frequently hinder the natural propagation of vibrations, which in turn retard their effectiveness as a means of the transportation of heat. The outcome influences the thermal conductivity of BiBro in future. [**?**, 50, 51].

The Fig. 10 illustrates the phonon density of states. The phonon(DOS) of BiBrO shows that there are sharp and large concentrations of vibration modes in the low-frequency part of the spectrum (1-4 THz), and then a clear phononic gap and a set of weaker high-frequency modes, extending between about 8.1 and 13 THz. The heavy atomic masses of Bi and Br can explain the dominance of low-frequency vibrations by reducing vibrational frequencies based on the lattice dynamical

principles $\omega \propto \sqrt{\frac{k}{m}}$, therefore, increasing the contribution of acoustic and low-energy optical phonons. The division of the low and high-frequency space points to the decoupling of the lattice dynamics, where the higher-frequency modes are probably related to the lightest vibrations involving oxygen and the tightest bond strength. Dynamical stability of the crystal structure can be established by the absence of imaginary frequencies. A bimodal phonon distribution is an indicator of constrained phonon group velocities and increased phonon scattering, which can be of benefit in lowering the thermal conductivity of the lattice, and thus make the material potentially useful in thermoelectric and thermal insulation [52, 53].

Lattice thermal conductivity is a measure of the efficiency of the heat conduction through a substance owing to lattice vibration, specifically phonons. Phonons are the main carriers of thermal energy in semiconductors and insulators, as display in Fig. 11(a) [54]. At a temperature of 200K, the lattice usually reaches a maximum of 4.4 W/m.K, this is because the phonon population rises due to normal phonon scattering (N-process) and does not disrupt heat flow much, as well as because of the high group velocity. At elevated temperatures, a significant portion of the thermal energy is carried by high-frequency phonons, which become increasingly active, and the Umklapp scattering (U-process) dominates, phonons interact strongly and lose momentum, which reduces their capacity in conducting heat. Conductivity of heat is consequently lowered [55]. Studies indicate that phonons significantly affect the transfer of heat in various 2D layer material, as demonstrated by research on other 2D layer sructure. [56, 57]. The BiBrO exhibits weak lattice thermal conductivity, which is attributed to the material properties that limit the phonon transport. Due to the presence of the heavy Bi element, atom vibrations occur at very slow rates, ensuring that group phonon velocities are reduced. This leads to reduced efficiency in the transport of heat. In short, BiBrO has a moderate heat capacity poor thermal conductivity of the lattice, rendering it a good thermal insulator.

Thermal transport is governed by the group velocity because the lattice thermal conductivity is proportional to the product of the phonon group velocity and the heat capacity. When the temperature rises, the lattice becomes softer, and as a result, the group velocity of phonons reduces, leading to lower lattice thermal conductivity, the trend of this behavior is reflected well based on the trends observed in BiBrO material, as can be seen in Fig. 11 [58, 59]. Phonon group velocities are large in the low-frequency regime (acoustic), indicating a fast propagation of the respective vibrational modes inside the BiBrO structure, which corresponds well to the speed of sound in the material. Conversely, at frequencies between (1-2) THz, the phonon group velocity remains mostly constant. This indicates that vibrational speeds stay relatively steady or increase gradually in this high-frequency range, the atoms participate in highly localized 'rattling' motions. The energy remains trapped there temporarily, which reduces thermal conductivity. Overall, the thermal properties of BiBrO make it an interesting candidate in many thermal management applications, especially when heat absorption and insulation play the most crucial role.

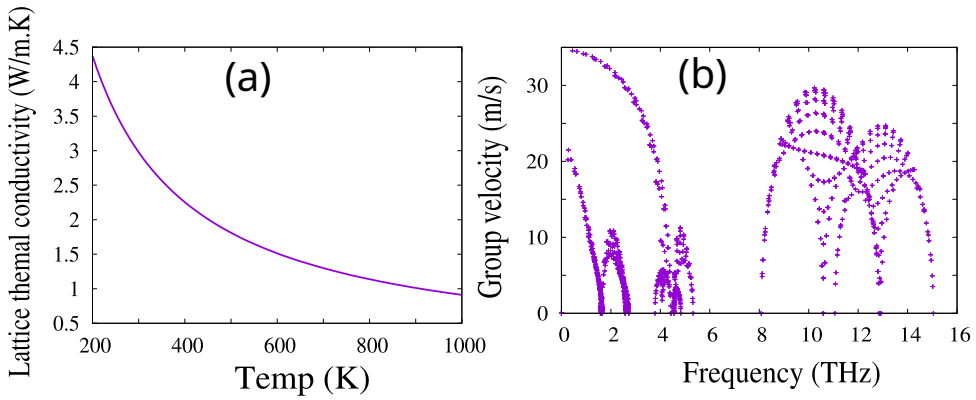

Figure 11. Lattice thermal conductivity (a),and Group velocity (b) in 2D BiBrO .

4. CONCLUSIONS

This study provides a thorough first-principles investigation of BiBrO's structural, stability, electronic characteristics, lattice dynamics, thermal stability, and optical characteristics. According to the band stracture calculation, the material has an indirect band gap of 2.42 eV, making it suitable for usage as a semiconductor. The lattice dynamical analysis demonstrates that there do not exist imaginary phonon frequency, and AIMD calculation prove that the structure remains stable under thermal condition, showing good dynamical and thermal stability. The considerable contribution of low-frequency vibrational modes in the phonon density of states suggests that lattice vibrations are efficiently dispersed and dissipated, resulting in increased material stability. In addition to these properties, the high optical response in the visible and ultraviolet regions along with the high absorption coefficient highlights its significant potential in the application in solar energy collection and optoelectronics. BiBrO exhibits excellent heat capacity, which is (24.66 J/K.mol per atom). As a result, the heat capacity remains reach the Dulong-Petit limit even at moderate temperatures. BiBrO's comparatively low lattice thermal conductivity implies that it is a good thermal insulator, since lower phonon-mediated heat transfer

improves its capacity to inhibit thermal diffusion. We discovered that the BiBrO has numerous applications in significant domains like as solar energy, energy conversion and thermal management applications.

5. ACKNOWLEDGMENT

The University of Sulaimani provided assistance for this research. The Computational Science Laboratory, Research and Development Center, University of Sulaimani, provided computational resources.

ORCID

Yadgar Hussein Shwan, https://orcid.org/0000-0002-0020-253X

REFERENCES

[1] D. Golberg, Y. Bando, Y. Huang, T. Terao, M. Mitome, C. Tang, and C. Zhi, "Boron nitride nanotubes and nanosheets," ACS nano, **4**(6), 2979-2993 (2010). https://doi.org/10.1021/nn1006495

[2] N. R. Abdullah, B. J. Abdullah, and V. Gudmundsson, "Modeling the electronic, phonon, magnetic, thermal, mechanical, and optical properties of a hybrid B3C2N3 nanosheet in the context of a bc6n single layer," Materials Science in Semiconductor Processing, **180**, 108581 (2024). https://doi.org/10.1016/j.mssp.2024.108581

[3] A. V. Kretinin, Y. Cao, J.-S. Tu, G. Yu, R. Jalil, K. S. Novoselov, S. J. Haigh, *et al.*, "Electronic properties of graphene encapsulated with different two-dimensional atomic crystals," Nano letters, **14**(6), 3270-3276 (2014). https://doi.org/10.1021/nl5006542

[4] P. Avouris, "Graphene: electronic and photonic properties and devices," Nano letters, **10**(11), 4285–4294 (2010). https://doi.org/10.1021/nl102824h

[5] P. Miró, M. Audiffred, and T. Heine, "An atlas of two-dimensional materials," Chemical Society Reviews, **43**(18), 6537–6554 (2014). https://doi.org/10.1039/C4CS00102H

[6] M. Xu, T. Liang, M. Shi, and H. Chen, "Graphene-like two-dimensional materials," Chemical reviews, **113**(5), 3766-3798 (2013). https://doi.org/10.1021/cr300263a

[7] D. Deng, K. Novoselov, Q. Fu, N. Zheng, Z. Tian, and X. Bao, "Catalysis with two-dimensional materials and their heterostructures," Nature nanotechnology, **11**(3), 218–230 (2016). https://doi.org/10.1038/nnano.2015.340

[8] Q. H. Wang, K. Kalantar-Zadeh, A. Kis, J. N. Coleman,and M. S. Strano, "Electronics and optoelectronics of two-dimensional transition metal dichalcogenides," Nature nanotechnology, **7**(11), 699–712 (2012). https://doi.org/10.1038/nnano.2012.193

[9] J. He, S. Ma, P. Lyu, and P. Nachtigall, "Unusual Dirac half-metallicity with intrinsic ferromagnetism in vanadium trihalide monolayers," Journal of Materials Chemistry C, **4**(13), 2518-2526 (2016). https://doi.org/10.1039/C6TC00409A

[10] W.-B. Zhang, L.-J. Xiang, and H.-B. Li, "Theoretical perspective of energy harvesting properties of atomically thin BiI 3," Journal of Materials Chemistry A, **4**(48), 19086–19094 (2016). https://doi.org/10.1039/C6TA06806E

[11] N. F. Coutinho, R. B. Merlo, N. F. Borrero, and F. C. Marques, "Thermal evaporated bismuth triiodide (BiI3) thin films for photovoltaic applications," MRS advances, **3**(55), 3233–3236 (2018). https://doi.org/10.1557/adv.2018.405

[12] Q. Wei, J. Chen, P. Ding, B. Shen, J. Yin, F. Xu, Y. Xia, and Z. Liu, "Synthesis of easily transferred 2D layered BiI3 nanoplates for flexible visible-light photodetectors," ACS applied materials & interfaces, **10**(25), 21527–21533 (2018). https://doi.org/10.1021/acsami.8b02582

[13] F. Ma, M. Zhou, Y. Jiao, G. Gao, Y. Gu, A. Bilic, Z. Chen, and A. Du, "Single layer bismuth iodide: computational exploration of structural, electrical, mechanical and optical properties," Scientific reports, **5**(1), 17558 (2015). https://doi.org/10.1038/srep17558

[14] Y. Zhang, P. Zhang, Y. Lan, L. Zhang, J. Yan, and X. Su, "Bismuth oxybromide photocatalysts for CO_2 reduction: modification methods, bottlenecks, and optimization strategies," Chemical Communications, **62**(2), 2877-2895 (2026). https://doi.org/10.1039/d5cc06774j

[15] I. H. Sabuj, Q. S. Hossain, S. S. Nishat, S. A. Jahan, M. Khan, U. S. Akhtar, M. S. Bashar, *et al.*, "Experimental and theoretical exploration of bismuth oxyhalide (BiOX, X= Cl, Br, I) nanoparticles in thermoelectric, optoelectronic, and photocatalytic applications," RSC advances, **16**(4), 3648–3661 (2026). https://doi.org/10.1039/D5RA07838E

[16] J. Zhang, Y. Liu, S. Xin, S. Lin, X. Zhang, J. Wang, X. Guo, *et al.*, "First-principles study of the effect of Bi content on the photocatalytic performance of bismuth bromide oxide-based catalysts," Physical Chemistry Chemical Physics, **27**, 3612-3621 (2025). https://doi.org/10.1039/D4CP04044A

[17] H. Fjellvåg, and P. Karen, "Crystal structure of $ScCl_3$ Refined from Powder Neutron Diffraction Data," Acta Chemica Scandinavica, **48**, 294–297 (1994). https://doi.org/10.3891/acta.chem.scand.48-0294

[18] X. Zhang, B. Li, J. Wang, Y. Yuan, Q. Zhang, Z. Gao, L.-M. Liu, and L. Chen, "The stabilities and electronic structures of single-layer bismuth oxyhalides for photocatalytic water splitting," Physical Chemistry Chemical Physics, **16**(47), 25854–25861 (2014). https://doi.org/10.1039/C4CP03166K

[19] A. Darmawan, E. Suprayoga, A. A. AlShaikhi, and A. R. Nugraha, "Thermoelectric properties of two-dimensional materials with combination of linear and nonlinear band structures," Materials Today Communications, **33**, 104596 (2022). https://doi.org/10.1016/j.mtcomm.2022.104596

[20] Y. H. Shwan, M. A. Ameen, A. S. Mahmood, DFT Study of the Stability, Electronic, Optical, and Thermal Properties of Two-Dimensional $BiBr_3$ Semiconductor, East European Journal of Physics (1) (2026) 191–202. https://doi.org/10.26565/2312-4334-2026-1-19

[21] P. Giannozzi, S. Baroni, N. Bonini, M. Calandra, R. Car, C. Cavazzoni, D. Ceresoli, *et al*., "Quantum espresso: a modular and open-source software project for quantumsimulations of materials," Journal of physics: Condensed matter B, **39**, 395502 (2009). https://doi.org/10.1088/0953-8984/21/39/395502

[22] A. Togo, and I. Tanaka, "First principles phonon calculations in materials science," Scripta Materialia, **108**, 1–5 (2015). https://doi.org/10.1016/j.scriptamat.2015.07.021

[23] J. P. Perdew, K. Burke, and M. Ernzerhof, "Generalized gradient approximation made simple," Physical review letters, **77**(18), 3865 (1996). https://doi.org/10.1103/physrevlett.77.3865

[24] Z.-Y. Zhao, Q.-L. Liu, and W.-W. Dai, "Structural, electronic and optical properties of $BiOX_{1-x}Y_x$ (X, Y= F, Cl, Br and I) solid solutions from DFT calculations," Scientific reports, **6**(1), 31449 (2016). https://doi.org/10.1038/srep31449

[25] X. He, Y. Wu, S. Liu, W. He, S. Li, G. Huo, L. Jiang, Y. Kapitonov, *et al*., "Large-scale ultrastable 2D inorganic molecular crystal $BiBr_3$ and heterostructures with superior photoluminescence enhancement," Advanced Functional Materials, **34**(39), 2403273 (2024). https://doi.org/10.1002/adfm.202403273

[26] W.-T. Ouyang, H.-T. Ji, Y.-Y. Liu, T. Li, Y.-F. Jiang, Y.-H. Lu, J. Jiang, and W.-M. He, "Tempo/O_2 synergistically mediated bibro-photocatalyzed decarboxylative phosphorylation of n-arylglycines," Chemistry–A European Journal, **30**(41), e202304234 (2024). https://doi.org/10.1002/chem.202304234

[27] A. Jehan, M. Husain, S. Bibi, N. Rahman, V. Tirth, A. Azzouz-Rached, M. Y. Khan, *et al*., "Insight into the structural, optoelectronic, and elastic properties of AuXF3 (X= Ca, Sr) fluoroperovskites: Dft study, Optical and Quantum Electronics, **55**(14), 1242 (2023). https://doi.org/10.1007/s11082-023-05394-4

[28] H. van Gog, W.-F. Li, C. Fang, R. S. Koster, M. Dijkstra, and M. van Huis, "Thermal stability and electronic and magnetic properties of atomically thin 2D transition metal oxides," NPJ 2D Materials and Applications, **3**(1), 18 (2019). https://doi.org/10.1038/s41699-019-0100-z

[29] Y. H. Shwan, M. A. Ameen, and A. S. Mahmood, "DFT study of electronic, optical, and thermodynamic properties of the 2D shape of Bi_44O_6 structure," Solid State Communications, **404**, 116095 (2025). https://doi.org/10.1016/j.ssc.2025.116095

[30] N. R. Abdullah, B. J. Abdullah, Y. H. Azeez, and V. Gudmundsson, "Exploring electronic, optical, and phononic properties of MgX (X= C, N, and O) monolayers using first principle calculations," arXiv preprint arXiv:2307.11041 (2023). https://arxiv.org/pdf/2307.11041

[31] Z. Zhang, Y. Xie, Y. Ouyang, and Y. Chen, "A systematic investigation of thermal conductivities of transition metal dichalcogenides," International Journal of Heat and Mass Transfer, **108**, 417–422 (2017). https://doi.org/10.1016/j.ijheatmasstransfer.2016.12.041

[32] T. Gunst, T. Markussen, K. Stokbro, and M. Brandbyge, "First-principles method for electron-phonon coupling and electron mobility: Applications to two-dimensional materials," Physical Review B, **93**(3), 035414 (2016). https://doi.org/10.1103/PhysRevB.93.035414

[33] N. R. Abdullah, B. J. Abdullah, and V. Gudmundsson, "DFT study of tunable electronic, magnetic, thermal, and optical properties of a Ga_2Si_6 monolayer," Solid State Sciences, **125**, 106835 (2022). https://doi.org/10.1016/j.solidstatesciences.2022.106835

[34] R. Arora, A. R. Barr, D. T. Larson, M. Pizzochero, and E. Kaxiras, "Engineering interfacial charge transfer through modulation doping for 2D electronics," Physical Review Materials, **9**(2), L021601 (2025). https://doi.org/10.1103/PhysRevMaterials.9.L021601

[35] J. Xie, Z. Zhang, D. Yang, D. Xue, and M. Si, "Theoretical prediction of carrier mobility in few-layer BC_2N," The Journal of Physical Chemistry Letters, **5**(23), 4073–4077 (2014). https://doi.org/10.1021/jz502006z

[36] J.-C. Tung, C.-H. Lee, P.-L. Liu, and Y.-K. Wang, "Electronic band structures of the possible topological insulator pb2bibro6 and pb2seteo6 double perovskite: An ab initio study," Applied Sciences, **12**(12), 5913 (2022). https://doi.org/10.3390/app12125913

[37] N. R. Abdullah, H. G. Hussein, and V. Gudmundsson, "Controlling electronic, magnetic, thermal, and optical properties of boron-nitrogen codoped strontium oxide monolayer: Activation of optical transitions in the vl region," arXiv preprint arXiv:2307.09173 (2023). https://arxiv.org/pdf/2307.09173

[38] S. Qi, Y. Zhang, R. Zhang, X. Liu, and H. Xu, "First-principles and experiment investigation of bi2o3/bi2wo6 heterojunctions," Colloid and Interface Science Communications, **44**, 100502 (2021). https://doi.org/10.1016/j.colcom.2021.100502

[39] T. L. Wakjira, K. Tadele, A. B. Gemta, and G. B. Kassahun, "Effect of tin doping and tin-bromine co-doping on electronic and optical properties of biocl crystal: density functional theory," Materials Research Express, **11**(6), 065903 (2024). https://doi.org/10.1088/2053-1591/ad549c

[40] W. L. Huang, "Electronic structures and optical properties of BiOX (X = F, Cl, Br, I) via DFT calculations," Journal of computational chemistry, **30**(12), 1882–1891 (2009). https://doi.org/10.1002/jcc.21191

[41] Y. H. Shwan, B. N. Ghafoor, and G. H. Hamasalih, "Optimization of surface plasmon resonance (spr) for gold/air interface by using kretschmann configuration," Engineering and Technology Journal, **40**(10), 1334-1341 (2022). https://doi.org/10.30684/etj.2022.132902.1151

[42] M. Barhoumi, and M. Said, "Electronic and optical properties of bismuth oxyhalides from ab initio calculations," Materials Science and Engineering: B, **264**, 114921 (2021). https://doi.org/10.1016/j.mseb.2020.114921

[43] M. Fang, Z. Wang, H. Gu, B. Song, Z. Guo, J. Zhu, X. Chen, *et al.*, "Complex optical conductivity of Bi_2Se_3 thin film: Approaching two-dimensional limit," Applied Physics Letters, **118**(19), (2021). https://doi.org/10.1063/5.0049170

[44] L. Chhana, B. Lalroliana, R. C. Tiwari, B. Chettri, D. P. Rai, L. Vanchhawng, L. Zuala, and R. Madaka, "Strain-modulated electronic and optical properties of monolayer and bilayer CdS: A DFT study," Journal of Electronic Materials, **51**(11), 6556–6567 (2022). https://doi.org/10.1007/s11664-022-09897-w

[45] T. L. Wakjira, K. Tadele, A. B. Gemta, and G. B. Kassahun, "Electronic, optical, phonon, and thermodynamic properties of bismuth oxyhalides for photocatalysis application using density functional theory," Discover Materials, **4**(1), 56 (2024). https://doi.org/10.1007/s43939-024-00131-4

[46] A. M. Ganose, M. Cuff, K. T. Butler, A. Walsh, and D. O. Scanlon, "Interplay of orbital and relativistic effects in bismuth oxyhalides: BiOF, BiOCl, BiOBr, and BiOI," Chemistry of materials, **28**(7), 1980–1984 (2016). https://doi.org/10.1021/acs.chemmater.6b00349

[47] A. Ghaleb, and A. Ahmed, "Structural, electronic, and optical properties of sphalerite zns compounds calculated using density functional theory (DFT)," Chalcogenide Letters, 19(5), 309-318 (2022). https://doi.org/10.15251/CL.2022.195.309

[48] V. Márta, Z. Pap, E. Bárdos, T. Gyulavári, G. Veréb, K. Hernadi, "Effect of urea as a shape-controlling agent on the properties of bismuth oxybromides," Catalysts, **13**(3), 616 (2023). https://doi.org/10.3390/catal13030616

[49] S. Praveen, S. Veeralingam, and S. Badhulika, "A flexible self-powered uv photodetector and optical uv filter based on β-Bi_2O_33/SnO_22 quantum dots schottky heterojunction," Advanced Materials Interfaces, **8**(15), 2100373 (2021). https://doi.org/10.1002/admi.202100373

[50] X. Tan, H. Shao, T. Hu, G. Liu, J. Jiang, and H. Jiang, "High thermoelectric performance in two-dimensional graphyne sheets predicted by first-principles calculations," Physical Chemistry Chemical Physics, **17**(35), 22872–22881 (2015). https://doi.org/10.1039/C5CP03466C

[51] Z.-X. Xie, L.-M. Tang, C.-N. Pan, Q. Chen, and K.-Q. Chen, "Ballistic thermoelectric properties in boron nitride nanoribbons," Journal of Applied Physics, **114**(14), 144311 (2013). https://doi.org/10.1063/1.4824750

[52] D. Singh, M. Sajjad, J. A. Larsson, and R. Ahuja, "Promising high-temperature thermoelectric response of bismuth oxybromide," Results in Physics, **19**, 103584 (2020). https://doi.org/10.1016/j.rinp.2020.103584

[53] Y. Li, J. Li, J. Tian, H. Liu, and J. Shi, "A first-principles study of 2d bi-based bioclbr, biocli, and biobri monolayers with ultralow lattice thermal conductivities for thermoelectric application," ACS Applied Nano Materials, **7**(13), 15086–15095 (2024). https://doi.org/10.1021/acsanm.4c01799

[54] J. J. Plata, P. Nath, D. Usanmaz, J. Carrete, C. Toher, M. de Jong, M. Asta, *et al.*, "An efficient and accurate framework for calculating lattice thermal conductivity of solids: Aflow-aapl automatic anharmonic phonon library," npj Computational Materials, **3**(1), 45 (2017). https://doi.org/10.1038/s41524-017-0046-7

[55] Y.-Y. Wu, Q. Wei, J. Zou, and H. Yang, "Ultra-low thermal conductivity and high thermoelectric performance of monolayer BiP_3: a first principles study," Physical Chemistry Chemical Physics, **23**(35), 19834–19840 (2021). https://doi.org/10.1039/d1cp01383a

[56] M. Markov, "Prediction of thermal conductivity and strategies for heat transport reduction in bismuth: an ab initio study," Ph.D. thesis, Université Paris Saclay (COmUE) (2016).

[57] M. Wang, and D. Han, "Thermal properties of 2d dirac materials MN_4 (M= Be and Mg): a first-principles study," ACS omega, **7**(12), 10812–10819 (2022). https://doi.org/10.1021/acsomega.2c00785

[58] Y. Luo, X. Yang, T. Feng, J. Wang, and X. Ruan, "Vibrational hierarchy leads to dual-phonon transport in low thermal conductivity crystals," Nature communications, **11**(1), 2554 (2020). https://doi.org/10.1038/s41467-020-16371-w

[59] A. Togo, "First-principles phonon calculations with phonopy and phono3py," Journal of the Physical Society of Japan, **92**(1), 012001 (2023). https://doi.org/10.7566/jpsj.92.012001

ПОГЛИБЛЕНЕ ДОСЛІДЖЕННЯ СТРУКТУРНИХ, СТАБІЛЬНИХ, ЕЛЕКТРОННИХ, ТЕРМОДИНАМІЧНИХ ТА ОПТИЧНИХ ХАРАКТЕРИСТИК ДВОВИМІРНОГО BiBrO НА ОСНОВІ ПЕРШОПРИНЦИПІВ

Ядгар Хуссейн Шван

Фізичний факультет, Коледж освіти, Університет Сулеймані, Сулеймания 46001, Курдистан, Ірак

Це дослідження використовує DFT в рамках GGA для проведення ретельного розрахунку стабільності, електронних властивостей, теплових характеристик та оптичних відгуків 2D BiBrO. Обчислена енергія утворення, разом з результатами розрахунку фононів та результатами AIMD, підтверджує стабільну структурну, динамічну та теплову стабільність системи BiBrO. 2D матеріал BiBrO демонструє напівпровідникову поведінку із забороненою зоною 2,42 еВ, що підтверджено аналізом електронної зонної структури. Аналіз оптичних властивостей BiBrO виявляє потужну взаємодію видимого та ультрафіолетового (УФ) світла, що підтверджує його застосування як пристрою накопичення сонячної енергії. Велика здатність BiBrO накопичувати теплову енергію зумовлена високою теплоємністю, оскільки BiBrO має більшу щільність фононних станів. Ентропія зростає пропорційно температурі, що означає додатковий атомний безлад і більш доступні мікроскопічні стани. Крім того, збільшення ентропії та плато теплоємності при високих температурах означають зміну до більш невпорядкованого стану, водночас забезпечуючи ефективне поглинання теплової енергії. Низька теплопровідність решітки та менша швидкість груп фононів BiBrO є характеристиками, які роблять матеріал корисним для теплоізоляції, зберігаючи при цьому структурну стабільність. Ці результати дають важливу інформацію щодо того, як BiBrO може бути використаний у системах накопичення енергії, а також як тепловий бар'єр.

Ключові слова: *2D BiBrO; DFT; електронні характеристики; теплопровідність решітки; оптичні характеристики; стабільність*